PAPER

Check for updates

Conversion of carbon black recovered from waste tires into activated carbon *via* chemical/microwave methods for efficient removal of heavy metal ions from wastewater†

M. M. El-Maadawy, [ID] [a] Amir A. Elzoghby, [ID] *[a] Ahmed M. Masoud, [ID] *[a] Alzahraa M. Eldeeb,[b] Ahmed M. A. El Naggar [ID] [c] and Mohamed H. Taha [ID] [a]

In this research study, recovered carbon black (rCB) was obtained *via* pyrolysis of waste tires. The obtained rCB was then converted into activated carbon species through both chemical treatment and microwave coupled with chemical treatment as a two-step activation process. The activated carbon obtained from chemical activation was denoted as C-AC, while that obtained from exposure to microwave followed by chemical activation was labeled as MC-AC. These two structures were consequently introduced as sorbents for the removal of cadmium ions from an aqueous solution. The structural characteristics of the introduced adsorbents were confirmed using various techniques, namely X-ray diffraction (XRD), Fourier-transform infrared (FTIR) spectroscopy, and energy-dispersive X-ray (EDX) spectroscopy. Additionally, textual features of these adsorbents were acquired *via* both scanning electron microscopy (SEM) and N_2 adsorption–desorption BET surface area analyses. These two structures were then introduced for Cd ion adsorption under different operating conditions. Particularly, the effect of pH, contact time, adsorbent dose, and metal ion concentration on the efficiency of adsorption was investigated. The 1maximum adsorption capacity was detected at a pH value of 5.0, a contact time of 30 min, a sorbent dose of 0.4 g L^{-1}, and an initial metal concentration of 50 mg L^{-1} using MC-AC, which exhibited nearly double the sorption capacity detected for C-AC. Kinetic studies indicated that the process of Cd(II) adsorption is perfectly described and fitted by the pseudo-second-order model. However, adsorption isotherms for the two adsorbents were found to match the Langmuir model, referring to the occurrence of uniform monolayer adsorption for the metal ions. Thermodynamic analysis demonstrated that the adsorption process was spontaneous and endothermic.

1. Introduction

In the past few decades, ecological contamination has posed an increasingly serious threat worldwide due to the introduction of persistent pollutants from diverse activities such as mining operations, paint industries, and agricultural runoffs. Continuous release of such pollutants has, in turn, led to the contamination of water, air, and soil.[1] One of these pollutants is cadmium metal, which is generally released into the environment by paint/pigment industries and is considered a toxic substance. Therefore, it has been necessary to find applicable cost-effective techniques to get rid of these toxins and ensure

the safety of flora and fauna.[2] However, big challenges are encountered by these industries to identify the most effective and economically beneficial methods to remove the traces of such heavy metals from waste samples.[3,4]

Various methods including precipitation, adsorption, oxidation, and nano-filtration have been extensively used for separating heavy metal ions from aquatic flows. Among those methods, adsorption has been well documented as an economical and effective technique for eliminating heavy metal ions from aqueous solutions. Thus, it is one of the most widely employed routes for such purposes owing to its adaptability, low cost, ease of processing, and limited generation of secondary wastes.[5–8]

Several structures have been utilized as adsorbents for the removal of heavy metals from wastewater; however, activated carbons (ACs) stand as one of the most efficient materials in such process. ACs offer several advantages including large inter-particulate surface area, controllable pore structure, thermo-stability, low acid/base reactivity, and highly modifiable

[a]*Nuclear Materials Authority, PO Box 530, El Maddi, Cairo, Egypt. E-mail: amirelzoghby33@gmail.com; chemmaso010@hotmail.com*

[b]*Chemistry Department, Faculty of Science, Mansoura University, Mansoura, Egypt*

[c]*Egyptian Petroleum Research Institute (EPRI), 1 Ahmed El-Zomor St., Nasr City, Cairo, Egypt*

† Electronic supplementary information (ESI) available. See DOI: https://doi.org/10.1039/d4ra00172a

surface chemistry.[9,10] Nevertheless, the use of commercial AC grades in wastewater remediation can add extra operating costs. Therefore, the utilization of affordable precursors, in particular biomass-based wastes such as agricultural and industrial remains, in the production of ACs has been strongly stimulated.[11] Recovered carbon black (rCB) from waste tires can be considered state-of-the-art source for the production of economically viable and efficient activated carbon (AC) as an adsorbent material.[12-14] Carbon black represents around 32%, by weight, of the waste tire composition; thus, its recovery and re-use in the production of ACs (as adsorbents) provide a proper solution for the problem of waste tire disposal.[15] However, such a structure of carbon, which is obtained *via* pyrolysis of the waste tire, may have a reduced porous structure and limited specific surface area.[16] Recent developments in the techniques of treating carbon black could help in the production of sustainable carbon species (with modified features) that could have a high potential for use as adsorptive materials.[17]

Microwave-assisted chemical treatment has been recently used as a substitute for traditional heating methods to produce activated carbon species.[18] Microwave provides uniform temperature, and direct and fast heating, which are its advantages over traditional heating.[19] High heating rates, no direct contact with the heated objects, small size of equipment, and reduced time/energy consumption are other benefits of heating by microwave, compared to conventional methods.[20] Therefore, the produced structures of activated carbon through the use of microwaves have demonstrated similar chemical and textural properties to those obtained *via* conventional heating methods; however, preparation time is significantly shortened.[21-24] Hence, microwave technology can offer a promising route for the production of activated carbon from different raw materials.

The objective of the current study is to investigate the behavior of waste tire sub-driven activated carbons toward the adsorption of dissolved cadmium ions in an aqueous solution. The novelty of this research work is based on recovering carbon black particles from waste tires followed by their conversion into species of activated carbons for use as new adsorbents in the removal of cadmium cations from wastewater samples. The combination of microwave, oxidizing agent, and chemical activator to generate activated carbon structures from rCB is considered another novelty of this study. The structural and textural features of the presented adsorbents in this study were determined using various techniques such as scanning electron microscopy (SEM), Brunauer–Emmett–Teller (BET) analysis, Fourier-transform infrared (FTIR) spectroscopy, and X-ray diffraction (XRD). Furthermore, the kinetics, thermodynamics, and isotherms for the process of Cd ion adsorption were analyzed and presented in the current research work.

2. Experimental

2.1. Materials

The utilized raw material to produce the activated carbon species was obtained from waste tires of vehicles, collected from a local company that is located in Cairo, Egypt. Analytical grade $CdSO_4$ purchased from Sigma-UK was used to prepare standard solutions (1000 mg L^{-1}) of Cd(II). NaOH and HNO_3, obtained from Adwic Ltd Egypt, were used to adapt the pH values of the Cd ion solutions.

2.2. Preparation of activated carbons

The production of activated carbons was done through a two-stage process: carbonization of the raw materials to obtain particles of recovered carbon black (rCB), as a first step, and activation of such carbon particles. In the carbonization stage, waste tires were cut into pieces, which were then dried at 110 °C for 24 h in an electric furnace to reduce their humidity. The dried pieces of the waste tire were then subjected to carbonization by heating to 500 °C in a pyrolysis unit.[25] After the pyrolysis process, rCB species were separated (*via* filtration) and washed using organic solvents to remove any attached organic impurities. Specifically, the acquired species of carbon were washed with *n*-hexane followed by the use of a methanol–benzene mixture (1 : 1 by weight). The washing step was carried out under vigorous stirring for 30 min, applying 1 g L^{-1} as the concentration of rCB in washing solvents. Subsequently, rCB particles were washed with deionized water and dried in a vacuum oven at 110 °C for 1 h to remove any residues of water molecules. The purified species of rCB next received activation *via* two routes which are as follows:

2.2.1 Chemical activation. This process was performed through wet-mixing of $ZnCl_2$ with rCB (applying a ratio of 2/1 w/w) followed by heating in a tube furnace (Nabertherm, Germany) at 500 °C for 1 h under N_2 flow at a rate of 50 mL min^{-1}, as reported earlier.[9] After activation, the produced carbon species were washed multiple times with 0.5 N HCl at a temperature of 85 °C. The particles of the activated carbon were then filtered and consecutively rinsed several times with distilled water until reaching a pH value of 7. After washing procedures, the collected carbon species were dehydrated under vacuum conditions at 110 °C for 2 h, and the obtained activated carbon was labeled as C-AC.

2.2.2 Microwave/chemical activation. In this process, rCB was suspended in hydrogen peroxide (using a ratio of 1/10 carbon to H_2O_2, by weight) inside a glass reactor, which was then located in a microwave cavity with a power input of 600 W and a frequency of 2.45 GHz for 15 min.[26] After activation, the produced carbon was washed multiple times with distilled water until a pH value of 6–7 was noticed. Consequently, the generated species of the activated carbon from microwave treatment received an additional chemical activation step with $ZnCl_2$, as described above.[9] The resulting activated carbon through combining microwave and chemical activation is labeled as MC-AC.

2.3. Characterization

A scanning electron microscope model JM-2100-XX, JEOL-Japan (offers magnification up to 35 000 times) was employed to explore the surface morphologies of the produced two carbon structures. Before being subjected to microscopy, the tested carbon samples were coated with a thin layer of gold to ensure high conductivity during the scanning process, which was

operated at 120 keV. The structural characteristics of both carbon samples were performed using an FTIR device, model Nicolet Is-10, USA, with a KBr disk. To prepare the samples for IR analysis, ~10–15 mg of carbon sample were added to mineral oil (3–4 drops). Then this mixture was grind in a mortar to form a thick paste. A small amount of the produced paste was placed on a salt plate, which was then covered by a second plate. Nitrogen adsorption–desorption measurements were carried out at 77.35 K using a Nova Touch LX4 Quantachrome, USA to determine the surface features of the carbon structures using a Brunauer–Emmett–Teller (BET) Barrett–Joyner–Halenda (BJH) methods. Before starting surface measurements, samples were degassed overnight at 200 °C under vacuum pressure of 10^{-4} Torre. A Raman spectrometer (BRUKER-SENTERRA, Germany) equipped with an integral microscope (Olympos) was utilized to further investigate the structures of carbon samples. The Raman device was operated using a He–Ne Laser beam at a wavelength of 533 nm.

2.4. Adsorption studies

A systematic study was conducted to investigate the impact of various operating parameters on the efficiency of Cd(II) uptake using the prepared activated carbon structures (C-AC and MC-AC). Contact time, pH, adsorbent dose, initial concentration of metal ions, and temperature are the experimentally investigated operational parameters. After each run of the experiment under different operating conditions, the solid phase (adsorbents carrying Cd ions) was initially segregated from the aqueous solutions using a Universal 320 centrifuge (operated at 2000 rpm) followed by its separation via filtration technique. Then, residual concentrations of Cd ions (mg L^{-1}) in the aqueous solutions were measured using a flame atomic absorption spectrophotometer (FAAS), PerkinElmer, USA. Based on the acquired data, the disposed amount of Cd(II) by the sorbents (q_e), the removal efficiency of the metal ions ($R\%$), and the distribution coefficient (K_d) were calculated using eqn (1)–(3), as described earlier.[27]

$$q_e = (C_o - C_e) \times \frac{V}{m} \tag{1}$$

$$R\% = \frac{(C_o - C_e)}{C_o} \times 100 \tag{2}$$

$$K_d = \frac{q_e}{C_e} \times 100 \tag{3}$$

where C_o and C_e (in mg L^{-1}) are the concentrations of metal ions initially and at equilibrium respectively, m (g) is the sorbent mass and V (L) is the volume of aqueous solution.

3. Results and discussions

3.1. Material characterizations

3.1.1 FTIR spectroscopy analysis. For carbon structures, FTIR is spectroscopy is one of the major techniques to identify and determine their functional groups. Phenols, alcohols, aldehydes, ketones, ethers, and carbonyl groups are the most common functional groups that can be generally found in activated carbon structures and significantly affect their performances as adsorbents.[28] Fig. 1 displays the FTIR spectra of the produced activated carbons (that are employed as adsorbents in the current study) either via chemical activation or microwave-combined chemical activation of recovered carbon black. A broad absorption peak attributed to O–H stretching modes of the –COOH, and phenolic OH groups in C-AC is detected at 3429 cm^{-1} (Fig. 1A). This absorption band was also observed for the second structure (MC-AC); however, it displayed less broadness, and intensity and was a bit shifted to be at 3421 cm^{-1} (Fig. 1B).

The observed differences between the two bands possibly resulted from the increase in the number of present OH groups, in the second structure, due to the process of double activation via microwave and chemical routes. Additionally, an absorption signal located in the range from 3000 to 2800 cm^{-1}, allocated for the C–H bond, could be detected in both activated carbon structures. The noticed peaks in the two structures showed similar shapes and locations, while they have different intensities. This noted variation is referred to as the strain stress in MC-AC species due to the use of various chemical reagents. This finding can be explained by conserving the present skeleton of hydrocarbon in raw feedstock (rCB) during the production of activated carbon structures by chemical activation either individually or in combination with microwave irradiation.

In the range between 1650 and 1000 cm^{-1}, the two AC structures showed three IR bands assigned to the C–O, S–O–C, and C–C vibrational bands. Nevertheless, the noticed peak at 1119 cm^{-1} was found to be less broad in the case of C-AC compared to MC-AC. This observation can be explained by the occurrence of stronger changes in the chemical structure during the process of producing MC-AC than in the case of C-AC. These chemical changes may include the formation of sulfonyl groups such as sulfone (–R–SO$_2$–R–) and sulfoxide (R–S=O).[29] The detection of such variations in the noted peaks verifies the occurrence of oxidative degradation of some chains of rCB structures during the H$_2$O$_2$- microwave treatment. Additional FTIR bands assigned to C–S and S–S bonds could be detected in between 600 and 680 cm^{-1}, for both structures. The observation of these signals can be explained by the existence of retained sulfur compounds in the produced activated carbon structures since the compounds of sulfur are present in the original raw materials (carbon black).

3.1.2 Surface area analysis. The surface characteristics of the two produced activated carbon structures (C-AC and MC-AC) were acquired by the N$_2$ adsorption–desorption method, as illustrated in Table 1, The BET-specific surface area (S_{BET}) of the activated carbon (MC-AC) was found to be approximately double the detected value of C-AC. Nevertheless, the total pore volume of the latter structure was slightly less than that of MC-AC. Moreover, the two structures showed a quite wide mesoporous nature; however, MC-AC could show narrower mesopores than those of C-AC. The differences between the surface features of the two AC structures can be explained by the varied routes of their reconstruction and rearrangements during the two different processes through the activation stage. In other
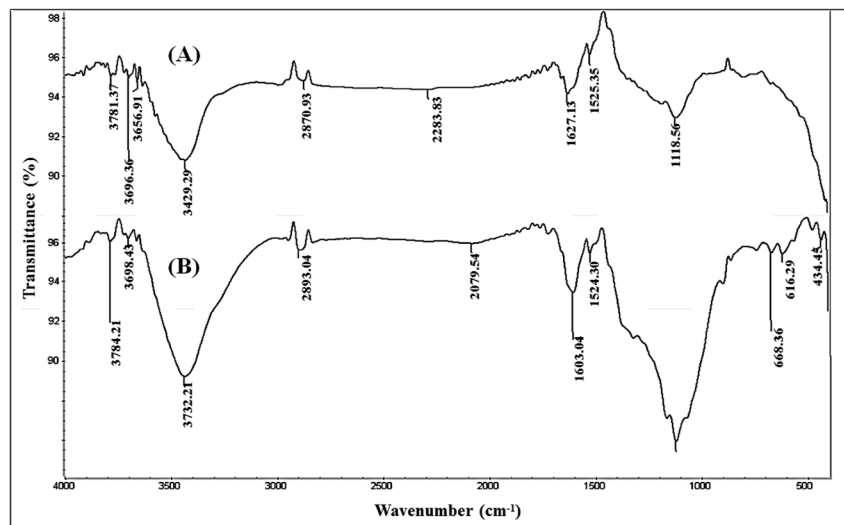
Fig. 1 FT-IR spectra of (A) C-AC and (B) MC-AC carbon species.

Table 1 Surface characteristics of C-AC and MC-AC carbon species

	Surface area ($m^2\ g^{-1}$)	Pore volume ($cm^3\ g^{-1}$)	Pore size (nm)
C-AC	86	0.042	19
MC-AC	154	0.048	12

words, it can be said that the combination of both microwave and chemical activation during the production of MC-AC could have a significant impact on the features of such carbon structure. Particularly, the use of double activation through preparing MC-AC could result in attaining stronger break-up of the long-chain carbon structures, leading to an obvious increment in its ultimate surface area value compared to C-AC. Additionally, the use of H_2O_2 during microwave activation could add charge species on the surfaces of the generated carbon particles. This could subsequently enhance the number of pores (pore volumes) as well as reduce their sizes in the case of MC-AC than in the case of C-AC. Hence, an increased specific surface area value could be obtained for the MC-AC structure.

3.1.3 Raman analysis. Raman spectroscopy is one of the techniques that is essentially utilized to identify carbon structures and to examine the chemical bond structure as well as the vibrational characteristics of sp^2-hybridized carbons.[30] For such structures, the D band and G band are two prominent features where the D band is known as the disarranged band, which is generally observed in all graphite-like carbons and gained from the hybridized vibrational modes based on their linkage with carbon edges.[31] Thus, the detection of such a band is an indication of the presence of structural defects.[7] Furthermore, the G band illustrates the level of graphitization and usually appears due to the hybridization of carbon (sp^2) as well as the enlarging mode in the C–C bond that is present in graphitic supplies.[32] The spectra of both C-AC and MC-AC samples (Fig. 2A and B) display the characteristic trait peaks of carbon materials

through observation of two bands at 1325 cm^{-1} (D band) and 1589 cm^{-1} (G band), which have fairly comparable intensities.[33]

The observation of relatively close intensities of these bands, in both AC samples, implies the non-amorphous and properly ordered structures. This finding is relevant to the I_D/I_G ratio, which is widely used to evaluate the level of structural disorder in carbon materials. This ratio is obtained by dividing the integrated intensity of the disorder band by the integrated intensity of the Raman-allowed band.[34] This ratio serves as an indicator of the number of structural defects and also measures the degree of exposure of edge planes, making it a frequently utilized measure for evaluating the level of structural order.[35] It is well established that a carbon structure with a high degree of defects is associated with a higher I_D/I_G ratio.[27] The I_D/I_G ratio of C-AC and MC-AC is slightly higher than 1, which indicates that both structures are of reasonable crystalline and ordered nature.[7]

3.1.4 SEM. The morphological features of both C-AC and MC-AC are respectively illustrated through the given SEM images in Fig. 3A and B. Both structures revealed properly uniform smooth morphologies with porous natures. However, the C-AC structure could show particles with various shapes of bigger sizes than those of MC-AC. Particularly, spherical, tetrahedral, and pentagon particles with sizes in the range of 50–70 microns could be observed for C-AC, while in the case of MC-AC, mostly spherical particles have a size of nearly 20 microns that could be detected. Moreover, MC-AC could display a larger number of pores than those noticed for the C-AC structure, showing that the double routes of activation had remarkably improved the surface appearance. The higher porosity of the MC-AC structure, owing to the detection of numerous cavities and uniform distribution of regularly shaped pores, than that of C-AC is in agreement with the previously illustrated surface area analysis. Based on the exhibited morphologies, the two presented structures obviously exhibit good potential to act as efficient adsorbents; however, MC-AC is
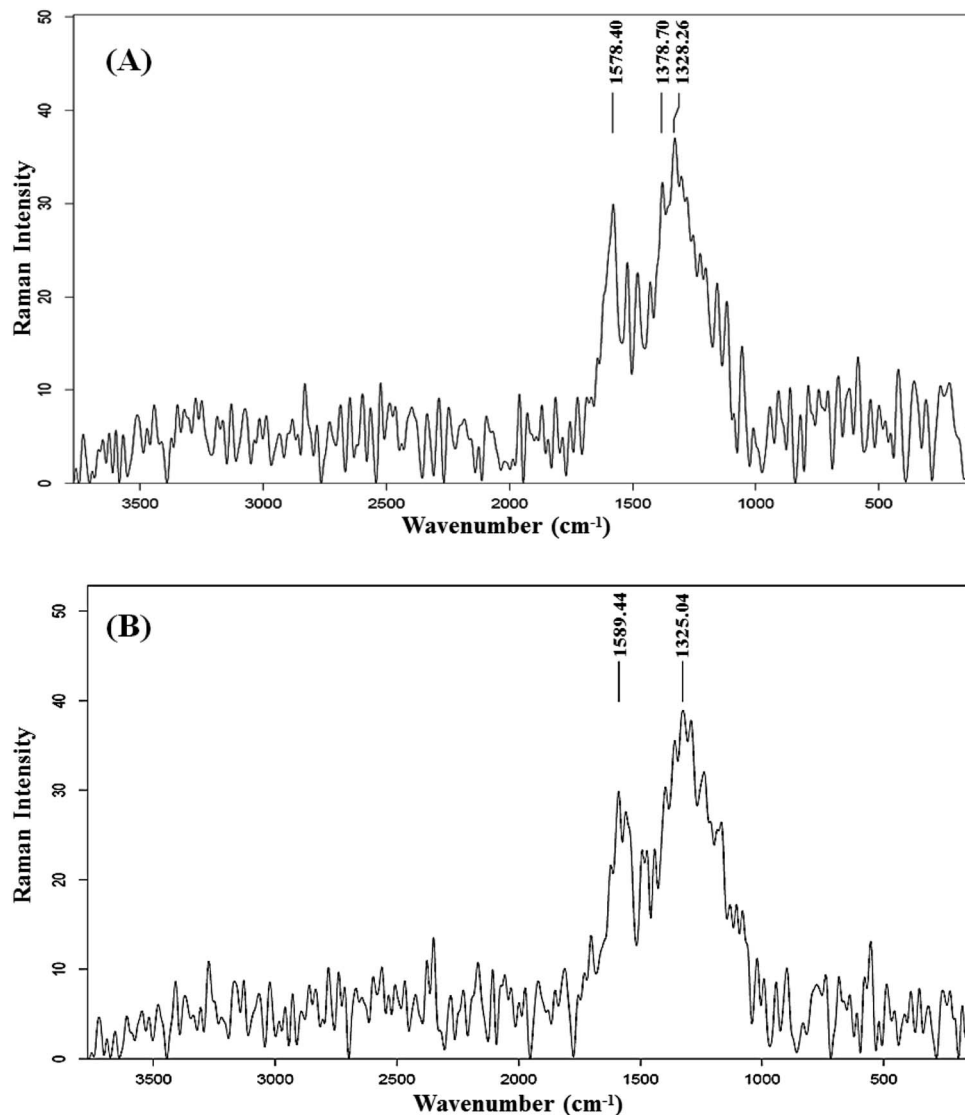
Fig. 2 Raman analysis of (A) C-AC and (B) MC-AC species.

expected to show a bit increased activity compared to the other structures.

The chemical compositions of the two presented activated carbon structures were further investigated through the given elemental analysis *via* the energy-dispersive X-ray (EDX) spectra shown in Fig. 3C and D for C-AC and MC-AC respectively. The two structures exhibited peaks indicative of carbon, oxygen, sulfur, zinc, and chlorine elements as main constituents. The detection of indicative signals for C, O, and S elements is attributed to their presence in the original chemical structure of rCB, which was utilized as the raw material for preparing the activated carbon structures. Furthermore, the observation of Zn and Cl in both structures refers to the use of zinc chloride as a chemical activator during the preparation of C-AC and MC-AC. Nevertheless, the weight% of the detected elements is quite different in the two investigated AC structures. In particular, 48, 55, 32.35, 12.1, 10.6 and 6.4 wt% were noted for C, O, Cl, Zn, and S elements respectively in the C-AC structure. These weight percentages were quite different in the case of the MC-AC structure, particularly, they were found to be (C, 43.25%), (O, 39.75%), (Cl, 11.5%), (Zn, 10%) and (S, 5.5%). The variations in acquired percentages are explained by the use of hydrogen peroxide as an activator reagent during the preparation of MC-AC. Therefore, the percentage of O elements could be subsequently increased in the composition of MC-AC than in C-AC. The increase in the O content of MC-AC had been compromised by slight drops in the noticed percentages for C, Cl, Zn and S elements.

3.1.5 XRD analysis. The structural features of the illustrated carbon structures, through this research study, were further examined *via* the given X-ray diffraction (XRD) patterns, as shown in Fig. 4A and B. Broad peaks in the range of 18–27° could be observed in the spectra of both samples, which are indicative of the presence of quite amorphous carbon structures. However, MC-AC could reveal less broadness than that detected in the case of the C-AC structure. This clearly could
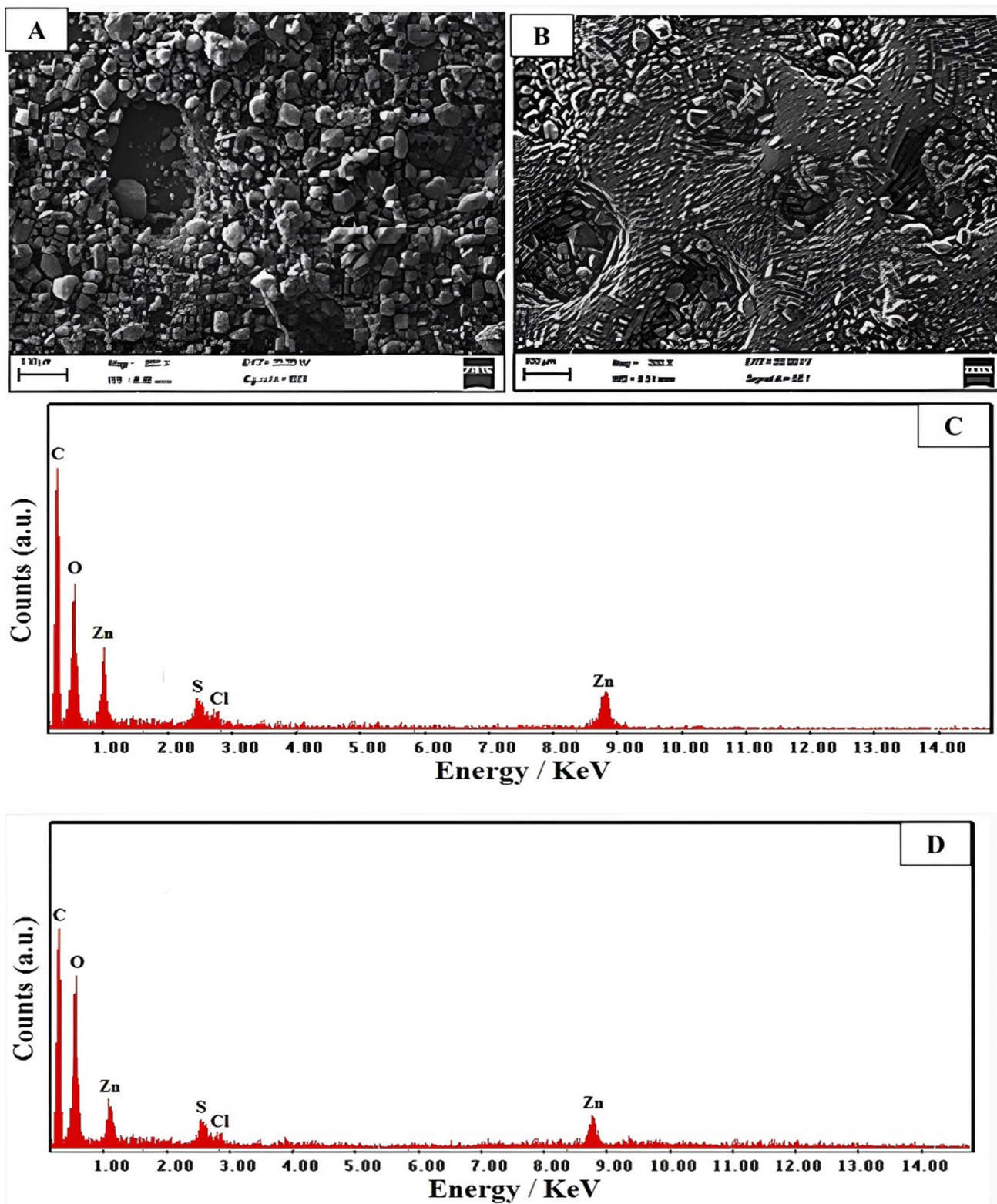
Fig. 3 Morphology of (A) C-AC and (B) MC-AC species. EDX analysis of (C) C-AC and (D) MC-AC species.

indicate that MC-AC is of better nature of crystallinity than C-AC, which is in good agreement with their previously discussed surface area analysis and surface morphologies. The given XRD spectra could also present two peaks at ∼26.78° and 42.17° corresponding to the (002) and (101) lattice planes of amorphous carbon. These peaks are normally assigned for the graphitic structure and characteristic of carbon materials, as reported by Poursorkhabi et al. 2020.[30]
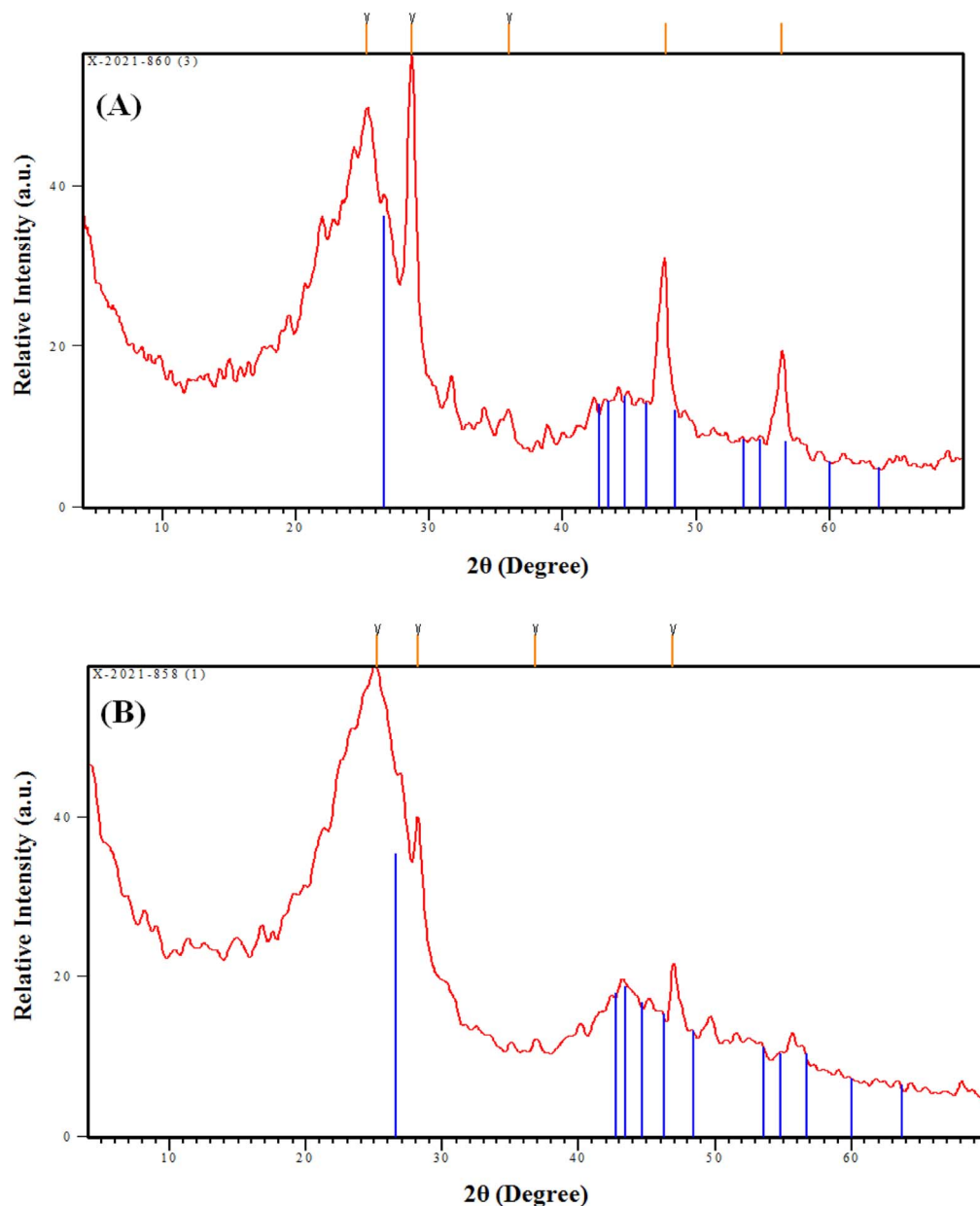
Fig. 4 XRD patterns of (A) C–AC and (B) MC–AC species.

3.2. Sorption investigation

In this section, the implementation of both carbon structures (C-AC and MC-AC) in the process of Cd(II) uptake from an aqueous solution was examined. The effect of various operating factors such as processing time, initial concentration, amount of carbon, and temperature on the adsorption process was tested. Additionally, sorption kinetics, isotherms, and thermodynamics were analyzed to obtain valuable data necessary for scaling up the experiments and designing the process effectively.

3.2.1. Effect of pH. The adsorption process is significantly influenced by the initial pH of solutions containing metal ions, as it affects the composition of metal ions in the solution and the characteristics of the adsorbent surface. The present work specifically investigates the dependence of the uptake percentage of Cd(II) ions using C-AC and MC-AC on the solution pH (2–9). The other variables were fixed at a sorbent dose of 5.0 g L^{-1}, room temperature, a shaking time of 240 min, and an initial concentration of 50 mg L^{-1}. The findings, illustrated in Fig. 5, demonstrate a rapid increase in the adsorption capacities of C-AC and MC-AC for Cd(II) within the boost of solution pH from 2.0 to 5.0. The maximum adsorption efficiency for Cd(II) was observed at pH 7.0, even though the rate of Cd(II) uptake increased more slowly as the initial pH increased from 5.0 to 7.0. C-AC and MC-AC demonstrated maximum Cd(II) adsorption efficiencies of 51.5% and 93.7% at solution pH 7.0, respectively. Furthermore, the corresponding maximum sorption capacity values were determined to be 5.2 mg g^{-1} for C-AC and 9.4 mg g^{-1} for MC-AC. Extending the solution pH to 9.0 deduced a negative impact on the sorption percentage.
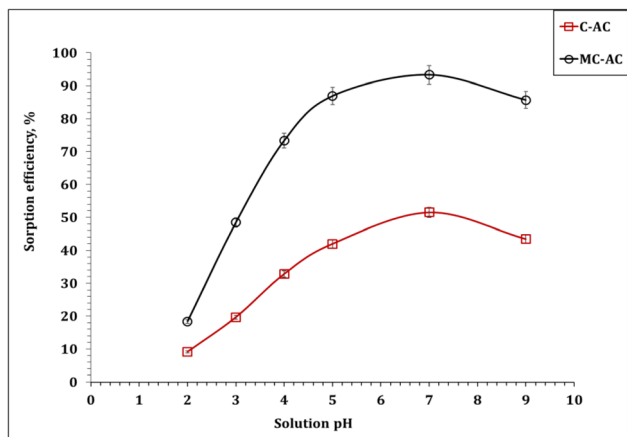
Fig. 5 Dependence of cadmium(II) ion uptake percentage on the solution pH (5.0 g sorbent L^{-1}; initial concentration: 50 mg L^{-1}; 240 min; room temperature).
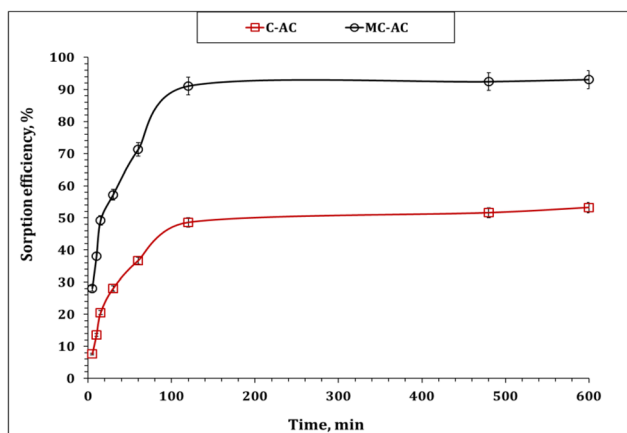

Fig. 6 Impact of stirring time of MB sorption percentage (pH 6.0; sorbent dose: 5.0 g L^{-1}; initial concentration: 50 mg L^{-1}; 25 °C).

The recognized behavior can be explained by the speciation of Cd(II) alongside the solution pH. Hence, the Medusa/Hydra software was applied to explore the variation in Cd(II) species

Table 2 Evaluated parameters of the applied kinetic equations

		C-AC	MC-AC
Lagergreen pseudo first-order	k_1 (min^{-1})	0.007	0.009
	$q_{e\ cal}$ (mg g^{-1})	3.0	3.9
	$q_{e\ exp}$ (mg g^{-1})	5.3	9.3
	R^2	0.82	0.79
Pseudo second-order	k_2 (min^{-1})	0.006	0.007
	$q_{e\ cal}$ (mg g^{-1})	5.5	9.5
	$q_{e\ exp}$ (mg g^{-1})	5.3	9.3
	h (mol g^{-1} h^{-1})	0.20	0.65
	$t_{1/2}$ (h)	27.9	14.7
	R^2	0.99	0.99

(50 mg L^{-1}) in aqueous solutions (0.1 M nitric acid) against the pH of the aqueous solution (Fig. S1†).[36] The anticipated results reveal that Cd(II) exists mainly as cationic species (Cd^{2+}) at acidic and neutral solution pH values, which indicate an extraordinary contest with the plenty of H$^+$ ions at low pH (acidic medium), resulting in the increasing retention of cadmium ions in the solution. However, as the pH gradually increased, the concentration of H$^+$ ions in the solution decreased, leading to a weakening of the competitive adsorption between H$^+$ ions and Cd(II), resulting in an increment in the sorption percentage.[37,38] In a prolonged solution treatment at pH 8, Cd(II) is predominantly in the form of Cd(OH)$_2$ (the insoluble species), which negatively influences the uptake percentage. In essence, the obtained results indicate that Cd(II) sorption is a pH-dependent process, which is consistent with the work previously reported in the literature.[3,39,40]

3.2.2 Effect of contact time. The performance of Cd(II) uptake using carbon-based materials (i.e. C-AC and MC-AC) as a function of shaking time was studied at different time intervals ranging from 5 to 600 minutes, while the rest of the parameters were fixed at a solution pH of 6, a sorbent dose of 5.0 g L^{-1}, an initial concentration of 50 mg L^{-1}, and a temperature of 25 ± 1 °C. The outcomes displayed in Fig. 6 reveal that, during the first 120 minutes of the experiment, both activated carbons demonstrated rapid binding of Cd(II) through adsorption. C-AC captured 48.6%
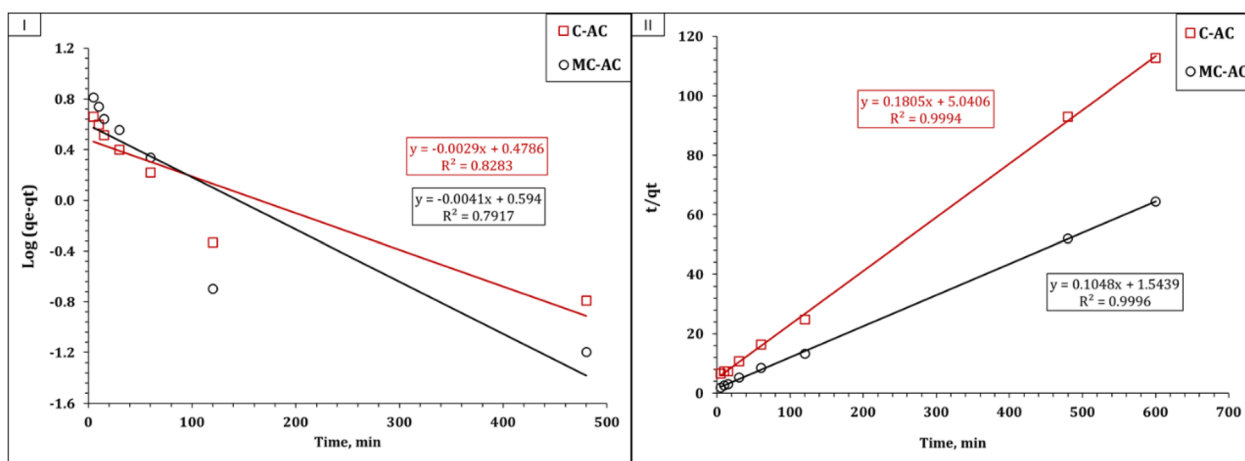

Fig. 7 Kinetic illustration of pseudo-first-order (I) and pseudo-second-order (II) models for the Cd(II) adsorption process.
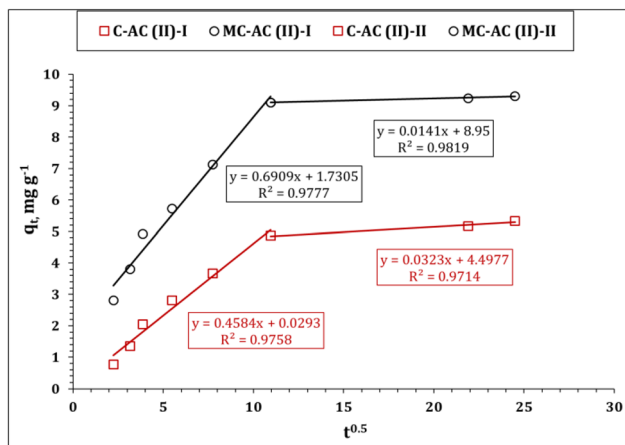
**Fig. 8** Morris–Weber model illustrating the sorption process.

Table 3 Evaluated parameters of the Morris–Weber kinetic model

Weber and Morris model		
Stage I		
k_i (mg g^{-1} min$^{-1/2}$)	0.46	0.69
C	0.03	1.73
R^2	0.97	0.97
Stage II		
k_i (mg g^{-1} min$^{-1/2}$)	0.03	0.01
C	4.5	9.0
R^2	0.97	0.98

(4.9 mg g^{-1}) of Cd(II), while MC-AC exhibited a higher adsorption efficiency of 91.1% (9.1 mg g^{-1}). However, beyond 120 minutes of shaking time, a sluggish Cd(II) removal process occurs. This attitude could be deemed to be due to the initial stage of sorption, there are numerous available surface sites for adsorption. Over time, the remaining vacant surface sites become difficult to occupy due to the repulsive forces between the cadmium ions in the aqueous phase and those adsorbed onto the solid surface.[41,42]

Understanding the kinetics of adsorption is crucial as it helps in designing and modeling the adsorption process. In this study, to investigate the adsorption kinetics of Cd^{2+} onto the synthesized carbons (CAC and MCAC), three kinetic models, namely, pseudo-first-order, pseudo-second-order, and intra-particle diffusion (Weber–Morris), were used. The main concept of the applied models could exist in the corresponding references. The linear forms of the applied kinetic models are displayed in Table S1.†[10,43,44] The coordination coefficient (R^2) equation is shown in Table S1† and used to explore the most suitable kinetic model.[10,43,44] The plot of the Lagergren model was exhibited as the variation in $\log(q_e - q_t)$ as a function of time (Fig. 7(I)), and the illustration of time/q_t against time (Fig. 7(II)) represents the pseudo-second-order model. The attained values of the kinetic parameters are declared in Table 2.

The deduced results in Table 2 elucidate that both applied sorbents exhibit the same kinetic profile, whereas the pseudo-second-order kinetic model for the Cd(II) uptake process
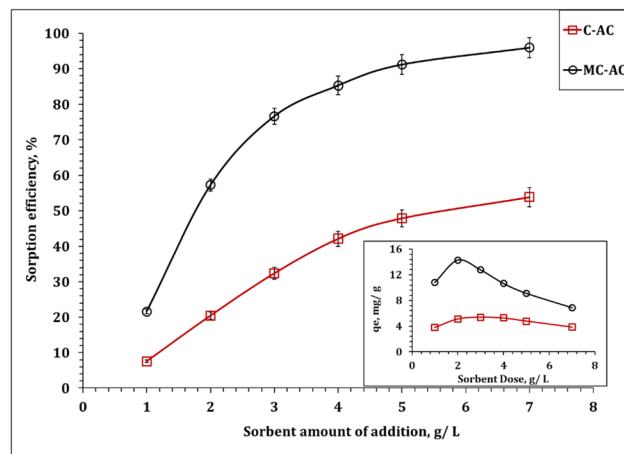
Fig. 9 Effect of sorbent dose on Cd(II) adsorption efficiency from aqueous solutions (pH: 6.0; 240 min; initial concentration: 50 mg L^{-1}; 25 °C).

exhibits excellent R^2 values (0.99). In addition, the experimental and calculated sorption capacities are so close (q_{eexp}: 5.3 and 9.3 mg g^{-1} for C-AC and MC-AC respectively; q_{ecal}: 5.5 and 9.5 mg g^{-1} for C-AC and MC-AC respectively). This indicates that the uptake process is chemisorption and involves electron sharing between the Cd(II) species and the C-AC and MC-AC function groups.[10,45] Luo *et al.*, and Tao *et al.*, reported that the uptake of cadmium(II) using biochars prepared from corncob and corn straw silage respectively obeyed the pseudo-second-order kinetic model.[39,46]

It is noteworthy that although both sorbents exhibit the same kinetic profile, the MC-AC carbonaceous sorbent displays a higher sorption capacity (q_e 9.5 mg g^{-1}), a higher initial sorption rate (0.65 mol g^{-1} h^{-1}), and a lower half equilibrium time (14.7 h) than those of the C-AC sorbent (q_e 5.5 mg g^{-1}, 0.65 mol g^{-1} h^{-1}, and 27.9 h respectively). This finding reflects that the double activation routes improve the sorption properties of the tire-based carbon than one activation route.

The Weber–Morris kinetic model was also applied to explore the mechanism of Cd(II) ion sorption using CAC and MCAC. The relation between q_t and time$^{0.5}$ (Weber and Morris plot) displays the mechanisms that control the sorption process, whether it is a solo (one-line segment with zero intercept) or multiple reaction mechanisms (several line segments).[10,43,44] Multiple sorption controlling mechanisms could be recognized from Fig. 8, whereas it exhibits a curve of numerous line segments. This indicates that the sorption process is performed through two stages: The first stage expresses the sorption process up to 120 min (reaction equilibrium). This stage is characterized by a rapid rate of reaction, which is due to the existence of free function groups on the carbonaceous material surface.[45,46] The other stage extends after equilibrium time and is described by a slow rate of reaction, caused by filling most of the adsorbent surface area holes.[45,46] It is worth noting from Table 3 that, the first stage of Cd(II) ion sorption process possesses lower constant C (boundary layer effect) and a higher rate of reaction than the second stage, which reflects that the sorption process
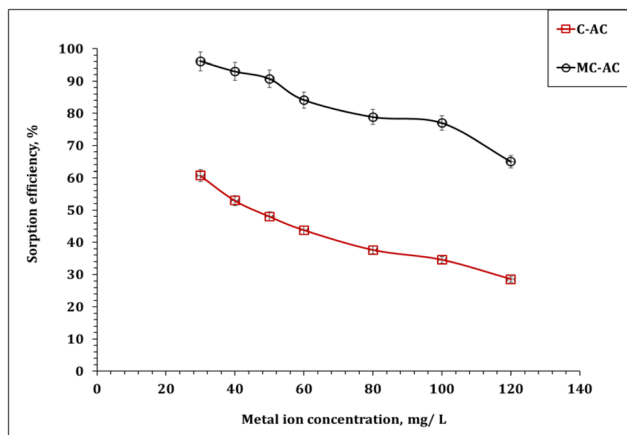
Fig. 10 Impact of the initial concentration of Cd(II) sorption (pH: 6.0; stirring time: 240 min; sorbent dose: 5.0 g L^{-1}; 25 °C).

Table 4 Evaluated variables of isotherm models

		C-AC	MC-AC
Freundlich isotherm model	$1/n$	0.34	0.29
	K_f (mg g^{-1})	1.6	5.6
	R^2	0.98	0.97
Langmuir isotherm model	q_m (mg g^{-1})	8.4	17.0
	K_L (L mg^{-1})	0.97	0.25
	R^2	0.99	0.98
Temkin isotherm	b_T (J mol^{-1})	1402.9	944.9
	B	1.77	2.95
	K_T (L g^{-1})	0.6	4.9
	R^2	0.97	0.95

in the first stage occurs at the sorbent surface (high rate of reaction), while in the second stage, the sorption process takes place inside the sorbent pores and the intra-particular diffusion is the controlling mechanism (low rate of reaction).[6,47]

3.2.3. Effect of adsorbent dosage. The influence of sorbent, in the range of 1–7 g L^{-1}, on Cd(II) uptake from aqueous solutions using C-AC and MC-AC sorbents was examined at room temperature, a shaking time of 240 min, an initial concentration of 50 mg L^{-1}, and a pH of 6.0. The results revealed that the sorbent dose increment led to a higher removal efficiency of Cd(II) ions (Fig. 9). This performance could be attributed to the boost in sorbent dose, offering a higher number of free surface active function groups, which increases the removal efficiency.[48] It is worth noting that the sorption capacity is negatively impacted as the sorbent dose increases (Fig. 9), which could be due to the existent Cd(II) ion solution being less equivalent to the
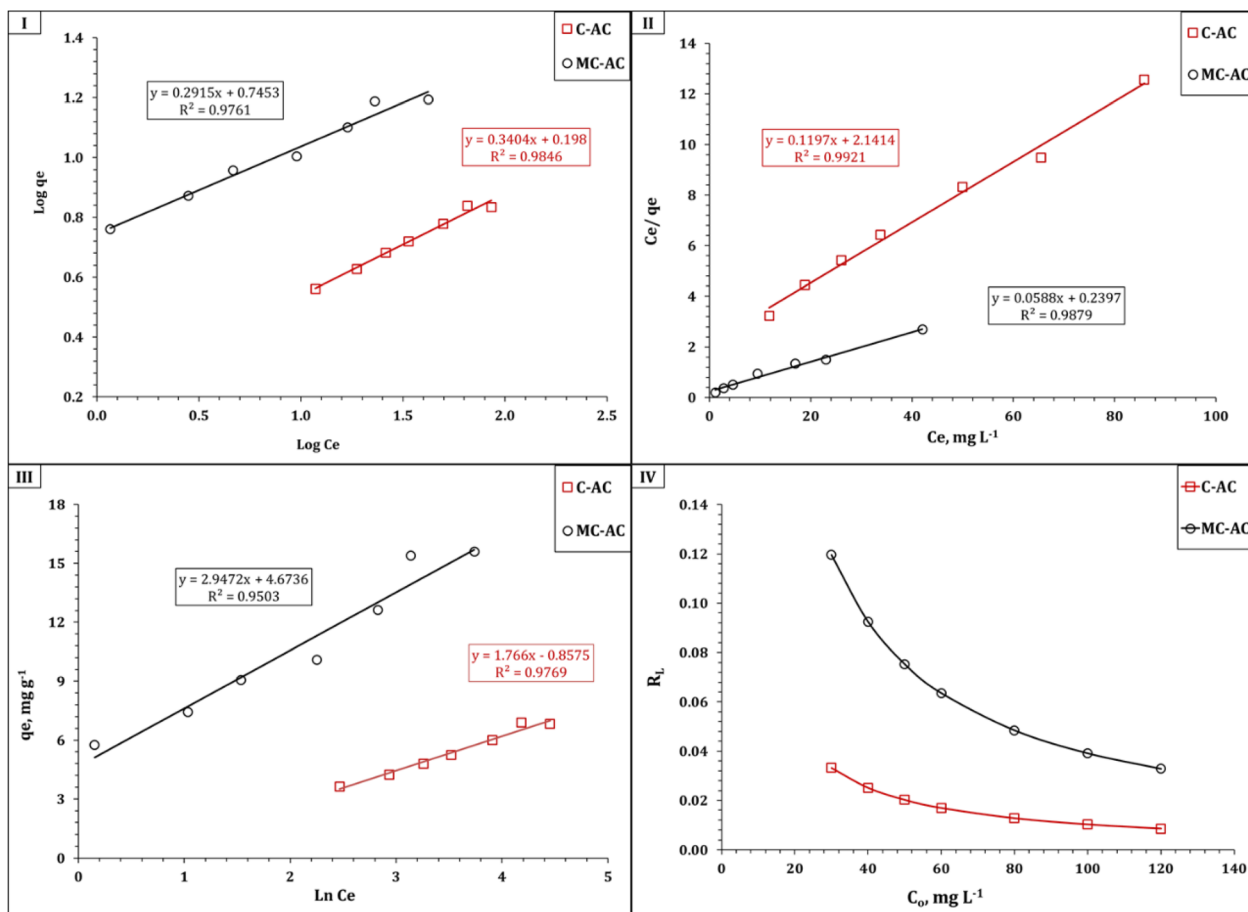

Fig. 11 Isotherm illustration of Freundlich (I), Langmuir (II), and Temkin (III) models for the Cd(II) sorption process, and separation factor R_L (IV).

Table 5 Sorption capacities of some previously reported carbon structures for Cd(II) removal

Sorbent type	Co (mg L^{-1})	Time (min)	pH	Temp (°C)	q_e (mg g^{-1})	Ref
Acrylonitrile modified Ac	20–200	1440	6.8	25	39.8	46
Modified AC generated rice straw	0–120	1440	10	25	8.1	53
Corn straw magnetic AC	10–150	360	6.0	25	16.4	47
Oyster shell AC	5–1000	1440	5.5	25	14.5	40
KOH-modified AC	0–20	1440	4.5	25	15.5	56
MnO$_2$-modified AC	2–50	1440	6.0	25	37.2	42
AC modified with shrimp bran	10–100	2880	6.0	20	41.1	49
Corn carbon fiber	20–300	720	4.0	25	21.3	36
Chemical activated carbon	**30–120**	**240**	**6.0**	**25**	**8.4**	**PW**[a]
Microwave/chemical-activated carbon					**17.0**	

[a] PW: present work.

existent sorbent mass, resulting in a decrease in the sorption capacity.[40]

3.2.4. Effects of initial concentrations. The assessment of Cd(II) removal efficiency as a function of initial concentration was conducted at a sorbent dose of 5.0 g L^{-1}, a shaking time of 240 min, a pH of 6.0, and a reaction temperature of 25 ± 1 °C, while the initial concentration varied from 30 to 120 mg L^{-1}. The displayed results (Fig. 10) deduce that the sorption efficiency radically reduced as the initial concentration increased, which could be attributed to that the applied sorbent mass is not equivalent to the Cd(II) ion concentration.[5,49] Katal et al.[50] also reported that a higher amount of pollutants were adsorbed at low concentrations.

The isotherm of Cd(II) uptake using C-AC and MC-AC sorbents could be profoundly dissected by analyzing the gained data using the following conventional isotherm models: Langmuir, Freundlich, and Temkin.[46–48] The main

concept of the applied models could exist in the corresponding references. The linear forms of the applied isotherm models are displayed in Table S1.†[10,51,52] The coordination coefficient (R^2) equation was applied to fit the applied models.[10,51,52] The variation in $\ln q_e$ against $\ln C_e$ (Fig. 11(I)) was applied to verify the Freundlich isotherm model, the Langmuir model plot (Fig. 11(II)) relates C_e/q_e versus C_e, and Fig. 11(III) displays the relation between q_e and $\ln C_e$ (Temkin isotherm model). The evaluated isotherm terms are presented in Table 4.

The data obtained from Table 4 indicate that the Langmuir model displayed the highest coordination coefficient for C-AC and MC-AC materials, which reflects that Cd(II) uptake occurs via a homogenous, uniform, and monolayer process.[10,53] This finding is consistent with the explored data from the SEM analysis for both sorbents, which reveal that both the structures have properly uniform smooth morphologies with porous natures (Fig. 2 and 3).
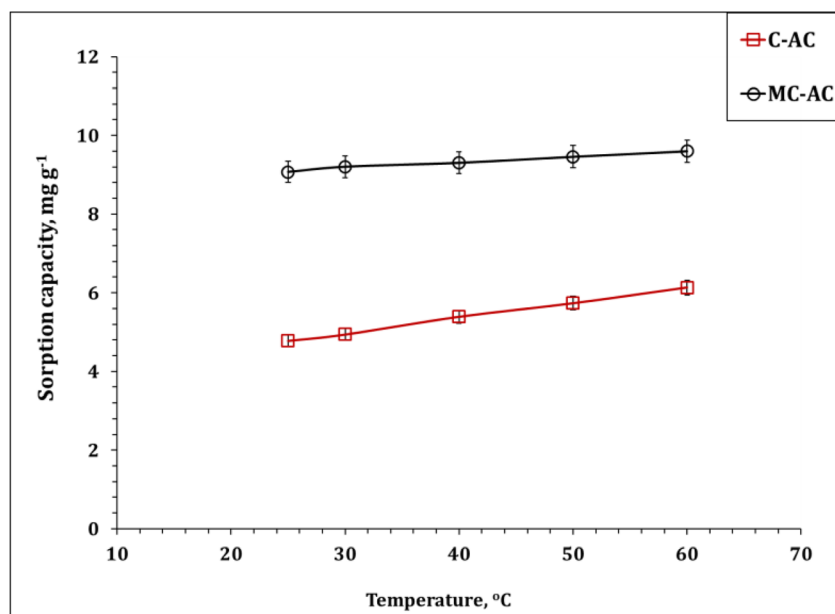

Fig. 12 Impact of the reaction temperature on Cd(II) sorption (pH: 5.0; stirring time: 240 min; sorbent dose: 5.0 g L^{-1}; initial Cd(II) concentration: 50 mg L^{-1}).

Table 6 Evaluated thermodynamic parameters

	ΔG (kJ mol^{-1})					ΔH (kJ mol^{-1})	ΔS (J mol^{-1} K^{-1})
	25 °C	30 °C	40 °C	50 °C	60 °C		
C-AC	−12.9	−13.3	−14.2	−15.0	−16.0	13.0	87.0
MC-AC	−18.8	−19.5	−20.5	−21.9	−23.5	20.2	130.7

The same isotherm performance (monolayer, uniform, and homogeneous process) was stated for Cd(II) removal from aqueous solutions using magnetic biochars modified with molybdenum disulfide (MoS$_2$@MBC),[47] titanium-modified ultrasonic biochars,[46] and corn straw magnetic biochar composites.[54]

The impact of double activation processes (microwave and chemical activation) than one activation process (chemical activation) for improving the sorption properties of the tire-based carbon could be recognized from the sorption capacity, whereas the double-activated carbon possesses almost two times the sorption capacity (17.0 mg g^{-1}) than the single-activated carbon (8.4 mg g^{-1}), as declared in Table 4. This higher sorption capacity of the MC-AC sorbent than that of the C-AC sorbent could be attributed to the double route activation processes yielding sorbents with mostly spherical particles and a large number of pores (Fig. 3), better nature of crystallinity (Fig. 4), and almost double surface area (Table 1), which reflects that the double activation route improves the sorption features of the produced activated carbon.

It is worth noting that the Freundlich and Temkin isotherm models exhibit proper coordination coefficients ($R^2 > 0.95$) for both applied sorbents, which indicate that the multilayer sorption process could take place during the sorption process,[10,53] and the physisorption nature for the Cd(II) uptake process could be explored from the value of the Temkin isotherm term heat of sorption (b_T).[55] The favorability of the uptake process could be figured out from the magnitude values of the Langmuir dimensional constant separation factor (R_L) and Freundlich constant $1/n$, whereas the sorption is favorable if the values of R_L and $1/n$ constants are between zero and one.[10,53] The values of R_L and $1/n$ anticipated in Fig. 11(IV) and Table 4 respectively obviously show that both terms have values less than one but higher than zero for both C-AC and MC-AC sorbents, which reflect a convenient process.[10,53]

The capacities of synthesized carbons for the adsorption of Cd^{2+} in this research work were compared with other materials reported in the literature, as presented in Table 5. The exhibited data indicate that the prepared sorbents in this study show potential as efficient materials for the uptake of cadmium since they showed good adsorption capacities, in comparison to those carbon structures that are previously reported in other studies. Nevertheless, some of these reported carbons revealed higher removal of Cd ions than that of C-AC and MC-AC. These increased activities could be referred to their higher surface area values, since they were produced form natural resources (agricultural waste), which have improved textural and structural properties than the recovered carbon black of waste tires. However, rCB

stands as a novel raw material for preparing activated carbon structures for use as efficient adsorbents in heavy metal recovery.

3.2.5. Effect of temperature and reaction thermodynamics. Fig. 12 illustrates the variations in the removal efficiencies of cadmium ions on C-AC and MC-AC at different temperatures (25–60 ± 1 °C). The anticipated data obviously showed that increasing the reaction temperature resulted in a slight improvement in the sorption capacity of both applied sorbents, which reveals an endothermic nature for Cd(II) sorption using both CAC and MCAC sorbents. This can be attributed to the temperature increment allowing the metal ions to overcome the energy barrier for diffusion or resist the concentration gradient.[5,6] It is important to properly assess the thermodynamic parameters to determine the impact of temperature on the adsorption capacity, as well as to gain insights into how the adsorption process affects the inherent energy and structure changes of the adsorbent. To accomplish the objective, the study determined three crucial thermodynamic terms: $\Delta G°$ (standard Gibbs free energy change), $\Delta H°$ (standard enthalpy change), and $\Delta S°$ (standard entropy change) using the thermodynamic equations presented in Table S1.†[28,36]

The dependence of the dimensionless distribution coefficient ($\log K_c$) on the reaction temperature ($1/T$) is illustrated (Fig. S2†) and used to explore the thermodynamic terms (Table 6). The deduced results confirm the endothermic nature of the sorption process, whereas $\Delta H°$ for both sorbents has positive values (13.0 and 20.2 kJ mol^{-1} for C-AC and MC-AC respectively).[5,6,47] It is worth noting that, $\Delta H° < 40$ kJ mol^{-1}, which indicates that the physisorption interaction mechanism with weak van der Waals bonds could be involved during the uptake process.[6,47] The spontaneous and feasibility uptake process could be recognized from the negative values of $\Delta G°$ for the entire temperature range.[46,47] The positive values of $\Delta S°$ for both sorbents indicate that the randomness decreases during the adsorption process.[46,47] The same thermodynamic performance (*i.e.* feasible, spontaneous, and endothermic system) was reported for the application of magnetic biochars modified with molybdenum disulfide (MoS$_2$@MBC),[47] corn straw magnetic biochar composites,[54] and titanium-modified ultrasonic biochars[46] for Cd(II) uptake from the aqueous solutions used.

3.2.6. Sorption mechanism. The interaction between the cadmium(II) species and activated carbons is mainly controlled by various variables such as the chemical structure and morphology of the applied carbon as well as the speciation of the cadmium ion in the aqueous solution.[45–47] Regarding these variables, different interaction mechanisms could be controlling the Cd(II) removal and wastewater remediation process.

These mechanisms involved precipitation, complexation, ion exchange, electrostatic interaction, and pore-filling.[56–59] Xu et al., 2013 and Wang et al., 2015 reported that a precipitation mechanism could take place during the Cd(II) uptake process between Cd(II) species and some anions released from the carbon surface such as OH^-, and CO_3^{2-}.[60,61] The cation exchange mechanism could also contribute to the adsorption mechanism by replacing cations such as Na^+, K^+, Mg^{2+}, and Ca^{2+} with Cd(II) ions, as mentioned by Tan et al. and Chang et al.[62,63] The removal of Cd(II) cation species could occur via electrostatic attraction mechanism, particularly using the sorbents with a negative surface charge (pH > pHpzc).[54] The activated carbon with a highly aromatic structure acts as a π-donor and Cd(II) acts as a π-acceptor, and hence, the cation–π interaction mechanism could be involved during the adsorption process.[48,64] The surface complexation interaction could be a crucial mechanism for Cd(II) uptake particularly for activated carbon with oxygen-containing functional groups.[60,65] Applied activated carbon with proper micropore structures and a large surface area could adsorb Cd(II) ions via the intra-particle diffusion mechanism.[57–59]

In the present study, Cd(II) speciation using the Medusa software gives a predominate cation species Cd^{2+} at pH < 8 (Fig. S1†). In addition, FTIR analysis (Fig. 1) for the prepared carbonaceous materials indicate the presence of oxygen-containing function groups such as –COOH and –OH, which give a negative charge to aqueous solutions. This reflects the effective contribution to the electrostatic attraction mechanism between the cationic Cd(II) species and the negatively charged sorbent surface during the uptake process. This finding is confirmed by the gained data from pH investigation (Section 3.2.1), which displayed that the adsorption percentage increases as the solution pH increases (H^+ ion concentration decreasing), as shown in Fig. 5.

Isotherm investigation shows that the adsorption process fits well with the Langmuir model (Table 4), which reflects a homogeneous, uniform, and monolayer sorption process. This finding is consistent with the surface morphology characterizations (Fig. 3 and 4), which declared that the prepared C-AC and MC-AC sorbents exhibit properly uniform smooth morphologies with porous nature.

Kinetic analysis displayed that the Cd(II) uptake process obeyed the pseudo-second-order model (Table 2), which elucidated that adsorption is a chemisorption process, and involved electron sharing between the Cd(II) species and the activated carbon function groups such as surface complexation and cation–π mechanisms.

Inner sphere surface complexation mechanism is involved during the Cd(II) adsorption process, whereas the applied sorbents possess several functional groups such as COOH, OH, C–O, S–O–C, $–R–SO_2–R–$ and R–S=O, which can form complexes with cadmium ions.[57–59] The cation–π interaction between the aromatic ring of the applied sorbents (electron donor) and the Cd(II) species (electron acceptor) could also take place during the removal process.

The kinetic analysis using the W–M model (Table 3) shows that the uptake process is controlled with multiple reaction mechanisms. Furthermore, the physical adsorption process could be also shared in the uptake of Cd(II) ions using C-AC and MC-AC, particularly at low available surface active sites (prolong equilibrium), whereas the prepared materials exhibit quite a wide mesoporous nature (Fig. 3 and 4). The thermodynamic investigation showed that $\Delta H° < 40$ kJ mol^{-1} (Table 6), which elucidated that the physisorption interaction mechanism with weak van der Waals bonds could be involved during the uptake process.[6,47]

3.3. Desorption and reusability investigation

Desorption and recycling investigations are important processes for optimizing and assessing wastewater remediation approaches. In this respect, the microwave and chemical activated tire (which exhibits the highest sorption tendency) loaded with Cd(II) ions was endured to a desorption process using 0.5 M of several acidic solutions (i.e. nitric, sulfuric, and hydrochloric acids), while the experimental conditions were kept at a shaking time of 240 min, a sorbent dose of 5 g L^{-1}, and room temperature. The achieved data (Table S2†) reveal that the hydrochloric acid solution was the most effective eluent for the Cd(II) desorption process, whereas about 93.7% desorption efficiency was deduced. The MC-AC sorbent was examined for five sequential sorption/desorption cycles. The achieved results indicated that after five cycles, only 7 and 9% of the sorption and desorption efficiencies respectively (Fig. S3†) were reduced from the fresh sorbent, which reflects a proper stability for the prepared activated carbon.

4. Conclusion

Waste rubber tires have been used to prepare carbonized and modified activated carbons (CAC and MCAC), and the products obtained have been characterized using a scanning electron microscope, an energy-dispersive X-ray spectrometer, an FTIR spectrophotometer, and an X-ray diffractometer. The resulting CAC and MCAC were tested as adsorbents for the removal of cadmium ions from the aqueous solution. The adsorption kinetics of the metal ion removal is fast at the beginning and then slowed down. The extent of the adsorption process is highly influenced by the pH of the solution, with greater adsorption observed at a pH of 5. After all, converting waste rubber tires into activated carbon is highly recommended, as it offers a doubly effective solution to environmental pollution. On the one hand, it provides a clean and sustainable way to dispose waste tires, and on the other hand, it offers an economically viable source of carbonaceous materials. The activated carbon obtained from waste tires can be used as an efficient adsorbent for the removal of heavy metals from aqueous solutions, as demonstrated in this study.

Author contributions

M. M. El-Maadawy: experimental operation, data interpretation, and writing – editing. Amir A. Elzoghby: methodology,

validation, data curation and interpretation, and writing – original draft, reviewing, and editing. Ahmed M. Masoud: conceptualization, supervision, and reviewing. Alzahraa M. Eldeeb: synthesis, characterization, data curation and interpretation, and writing – original draft. Ahmed M. A. El Naggar: methodology, investigation, data curation and interpretation, and writing – original draft, reviewing, and editing. Mohamed H. Taha: conceptualization, supervision, and reviewing.

Conflicts of interest

The authors of this manuscript confirm that they have no conflict of interest with any organization or person.

References

1 J. Briffa, E. Sinagra and R. Blundell, *Heliyon*, 2020, **6**, e04691.

2 S. Mitra, A. J. Chakraborty, A. M. Tareq, T. Bin Emran, F. Nainu, A. Khusro, A. M. Idris, M. U. Khandaker, H. Osman, F. A. Alhumaydhi and J. Simal-Gandara, *J. King Saud Univ., Sci.*, 2022, **34**, 101865.

3 R. Vidu, E. Matei, A. M. Predescu, B. Alhalaili, C. Pantilimon, C. Tarcea and C. Predescu, *Toxics*, 2020, **8**, 1–37.

4 E. W. Chu, J. R. Karr, *Reference Module in the Life Sciences*, 2017.

5 A. A. Younes, A. M. Masoud and M. H. Taha, *Int. J. Environ. Anal. Chem.*, 2023, **103**(20), 9117–9130.

6 A. A. Elzoghby, A. Bakry, A. M. Masoud, W. S. Mohamed, M. H. Taha and T. F. Hassanein, *J. Environ. Chem. Eng.*, 2021, **9**, 106755.

7 A. S. Morshedy, M. H. Taha, D. M. A. El-Aty, A. Bakry and A. M. A. El Naggar, *Environ. Technol. Innovation*, 2021, **21**, 101363.

8 M. M. Ali, S. A. Abedelmaksoud, M. H. Taha, A. M. A. El Naggar, A. S. Morshedy and A. A. Elzoghbi, *Radiochemistry*, 2020, **62**, 204–215.

9 Z. Heidarinejad, M. H. Dehghani, M. Heidari, G. Javedan, I. Ali and M. Sillanpää, *Environ. Chem. Lett.*, 2020, **182**(18), 393–415.

10 A. Morsy, M. H. Taha, M. Saeed, A. Waseem, M. A. Riaz and M. M. Elmaadawy, *Nucl. Sci. Technol.*, 2019, **30**, 1–11.

11 S. Afroze and T. K. Sen, *Water, Air, Soil Pollut.*, 2018, **229**, 1–50.

12 D. Ramutshatsha-Makhwedzha, A. Mavhungu, M. L. Moropeng and R. Mbaya, *Heliyon*, 2022, **8**, e09930.

13 N. Muttil, S. Jagadeesan, A. Chanda, M. Duke and S. K. Singh, *Appl. Sci.*, 2022, **13**, 257.

14 W. Chen, H. Feng, D. Shen, Y. Jia, N. Li, X. Ying, T. Chen, Y. Zhou, J. Guo and M. Zhou, *Sci. Total Environ.*, 2018, **618**, 804–809.

15 K. Kuśmierek, A. Świątkowski, T. Kotkowski, R. Cherbański and E. Molga, *J. Anal. Appl. Pyrolysis*, 2021, **157**, 105205.

16 C. G. Joseph, D. Krishniah, Y. H. Taufiq-Yap, M. Massuanna and J. William, *Adv. Mater. Res.*, 2015, **1107**, 347–352.

17 T. A. Saleh, V. K. Gupta and A. A. Al-Saadi, *J. Colloid Interface Sci.*, 2013, **396**, 264–269.

18 A. Kumar, Y. Kuang, Z. Liang and X. Sun, *Mater. Today Nano*, 2020, **11**, 100076.

19 W. Ao, J. Fu, X. Mao, Q. Kang, C. Ran, Y. Liu, H. Zhang, Z. Gao, J. Li, G. Liu and J. Dai, *Renewable Sustainable Energy Rev.*, 2018, **92**, 958–979.

20 B. S. Ondon, B. Sun, Z. Y. Yan, X. M. Zhu and H. Liu, *Appl. Water Sci.*, 2014, **4**, 333–339.

21 E. Çalişkan, J. M. Bermúdez, J. B. Parra, J. A. Menéndez, M. Mahramanlioǧlu and C. O. Ania, *J. Environ. Manage.*, 2012, **102**, 134–140.

22 S. Doja, L. K. Pillari and L. Bichler, *Renewable Sustainable Energy Rev.*, 2022, **155**, 111860.

23 V. K. Gupta, B. Gupta, A. Rastogi, S. Agarwal and A. Nayak, *J. Hazard. Mater.*, 2011, **186**, 891–901.

24 V. K. Gupta, A. Nayak, S. Agarwal and I. Tyagi, *J. Colloid Interface Sci.*, 2014, **417**, 420–430.

25 M. R. Yousuf, F. Mahnaz and S. R. Syeda, *Desalin. Water Treat.*, 2021, **213**, 441–458.

26 A. A. Ahmad, M. Al-Raggad and N. Shareef, *Carbon Lett.*, 2021, **31**, 957–971.

27 A. M. Masoud, M. Saeed, M. H. Taha and M. M. El-Maadawy, *Egypt. J. Chem.*, 2020, **63**, 721–741.

28 M. H. Taha, S. A. Abdel Maksoud, M. M. Ali, A. M. El Naggar, A. S. Morshedy and A. A. Elzoghby, *Int. J. Environ. Anal. Chem.*, 2019, **99**(12), 1211–1234.

29 K. Aoudia, S. Azem, N. Aït Hocine, M. Gratton, V. Pettarin and S. Seghar, *Waste Manage.*, 2017, **60**, 471–481.

30 V. Poursorkhabi, M. A. Abdelwahab, M. Misra, H. Khalil, B. Gharabaghi and A. K. Mohanty, *Front. Energy Res.*, 2020, **8**, 208.

31 C. Chailuecha, A. Klinbumrung, P. Chaopanich and R. Sirirak, *Mater. Today: Proc.*, 2021, **47**, 3525–3528.

32 B. Chaudhuri, S. Ghosh, B. Mondal and D. Bhadra, *Mater. Sci. Eng., B*, 2022, **275**, 115500.

33 F. Liu, H. Wang, L. Xue, L. Fan and Z. Zhu, *J. Mater. Sci.*, 2008, **43**, 4316–4322.

34 W. Qu, J. Liu, Y. Xue, X. Wang and X. Bai, *J. Appl. Polym. Sci.*, 2018, **135**, 45736.

35 K. L. Tan and K. Y. Foo, *Pet. Ind. Wastewater Adv. Sustain. Treat. Methods*, 2022, 185–203.

36 A. F. Abou-Hadid, U. A. El-Behairy, M. M. Elmalih, E. Amdeha, A. M. A. E. Naggar, M. H. Taha and A. E. M. Hussein, *Biomass Convers. Biorefin.*, 2023, **1**, 1–15.

37 Q. Wang, J. Shan Li and C. S. Poon, *J. Environ. Manage.*, 2019, **247**, 509–517.

38 T. C. Nguyen, P. Loganathan, T. V. Nguyen, J. Kandasamy, R. Naidu and S. Vigneswaran, *Environ. Sci. Pollut. Res. Int.*, 2018, **25**, 20430–20438.

39 Q. Tao, Y. Chen, J. Zhao, B. Li, Y. Li, S. Tao, M. Li, Q. Li, Q. Xu, Y. Li, H. Li, B. Li, Y. Chen and C. Wang, *Sci. Total Environ.*, 2019, **674**, 213–222.

40 W. Lian, H. Li, J. Yang, S. Joseph, R. Bian, X. Liu, J. Zheng, M. Drosos, X. Zhang, L. Li, S. Shan and G. Pan, *Bioresour. Technol. Rep.*, 2021, **15**, 100709.

41 M. H. Taha, *Environ. Sci. Pollut. Res. Int.*, 2021, **28**, 12475–12489.

42 Z. Wu, X. Chen, B. Yuan and M. L. Fu, *Chemosphere*, 2020, **239**, 124745.

43 L. Largitte and R. Pasquier, *Chem. Eng. Res. Des.*, 2016, **109**, 495–504.

44 E. D. Revellame, D. L. Fortela, W. Sharp, R. Hernandez and M. E. Zappi, *Clean. Eng. Technol.*, 2020, **1**, 100032.

45 M. H. Taha, A. M. Masoud, Y. M. Khawassek, A. E. M. Hussein, H. F. Aly and E. Guibal, *Environ. Sci. Pollut. Res.*, 2020, **27**, 31278–31288.

46 M. Luo, H. Lin, B. Li, Y. Dong, Y. He and L. Wang, *Bioresour. Technol.*, 2018, **259**, 312–318.

47 Z. H. Khan, M. Gao, W. Qiu and Z. Song, *Chemosphere*, 2020, **255**, 126995.

48 D. Xu, Y. Zhao, K. Sun, B. Gao, Z. Wang, J. Jin, Z. Zhang, S. Wang, Y. Yan, X. Liu and F. Wu, *Chemosphere*, 2014, **111**, 320–326.

49 W. Yin, C. Zhao and J. Xu, *Environ. Sci. Pollut. Res.*, 2019, **26**, 37092–37100.

50 R. Katal, M. S. Baei, H. T. Rahmati and H. Esfandian, *J. Ind. Eng. Chem.*, 2012, **18**, 295–302.

51 M. A. Al-Ghouti and D. A. Da'ana, *J. Hazard. Mater.*, 2020, **393**, 122383.

52 N. Ayawei, A. N. Ebelegi and D. Wankasi, *J. Chem.*, 2017, **2017**, 3039817.

53 S. Wang, N. Wang, K. Yao, Y. Fan, W. Li, W. Han, X. Yin and D. Chen, *Sci. Rep.*, 2019, **9**, 1–13.

54 Z. H. Khan, M. Gao, W. Qiu, M. S. Islam and Z. Song, *Chemosphere*, 2020, **246**, 125701.

55 A. M. Masoud, A. A. El-Zahhar, A. M. A. El Naggar, A. I. Zahran, G. A. A. Al-Hazmi and M. H. Taha, *Radiochim. Acta*, 2023, **111**, 105–115.

56 S. Bashir, J. Zhu, Q. Fu and H. Hu, *Environ. Sci. Pollut. Res.*, 2018, **25**, 11875–11883.

57 X. Cui, S. Fang, Y. Yao, T. Li, Q. Ni, X. Yang and Z. He, *Sci. Total Environ.*, 2016, **562**, 517–525.

58 Y. Deng, S. Huang, C. Dong, Z. Meng and X. Wang, *Bioresour. Technol.*, 2020, **303**, 122853.

59 B. T. Iber, V. T. Okomoda, S. A. Rozaimah and N. A. Kasan, *Bioresour. Technol. Rep.*, 2021, **15**, 100702.

60 X. Xu, X. Cao and L. Zhao, *Chemosphere*, 2013, **92**, 955–961.

61 Z. Wang, G. Liu, H. Zheng, F. Li, H. H. Ngo, W. Guo, C. Liu, L. Chen and B. Xing, *Bioresour. Technol.*, 2015, **177**, 308–317.

62 L. Tan, Z. Ma, K. Yang, Q. Cui, K. Wang, T. Wang, G. L. Wu and J. Zheng, *Sci. Total Environ.*, 2020, **699**, 134223.

63 R. Chang, S. P. Sohi, F. Jing, Y. Liu and J. Chen, *Environ. Pollut.*, 2019, **254**, 113123.

64 H. N. Tran, S. J. You, A. Hosseini-Bandegharaei and H. P. Chao, *Water Res.*, 2017, **120**, 88–116.

65 X. Cui, H. Hao, C. Zhang, Z. He and X. Yang, *Sci. Total Environ.*, 2016, **539**, 566–575.